AMAS Workshop on Orthopaedic Biomechanics
OBM'02 – (pp.293–332) – Wrocław, September 1-4, 2002.

Problems of heat transfer in orthopaedic biomechanics

M. STAŃCZYK and J. J. TELEGA

Institute of Fundamental Technological Research
Świętokrzyska 21, 00-049 Warszawa, Poland
mstan@ippt.gov.pl
jtelega@ippt.gov.pl

1. Introduction

The aim of this contribution is to present thermal problems specific to orthopaedics. One can identify them as the heat transfer phenomena taking place during and after orthopaedic operations in the direct vicinity of the operation site. The investigation of these processes is important for the following reasons:

- development of 'thermally safe' surgical procedures such as implant fixation, bone drilling etc.,
- manufacturing of implants that have better thermal and tribological properties,
- assessment of the properties of the existing prosthetic systems, their working temperatures and heat-accelerated wear rates.

The considered heat loads should be distinguished and characterized by the time duration and the intensity of the heat source. In fact those two factors are most important for survival of the living tissue. Before we embark on more quantitative analysis, let us present a simple yet illustrative thermal tissue damage criterion, involving temperature and duration, provided by Sapareto and Dewey [50]. These authors introduced the temperature of 43°C as a 'common denominator' for all isothermic treatments. The *equivalent time at* $45°\,C$, t_{43} is calculated as follows, after [50]:

$$t_{43} = t\,R^{(43-T)} \tag{1.1}$$

where t is treatment duration and T – its temperature. The number R is equal to 0.5 for temperatures greater than 43°C and equal to 0.25 for temperatures below 43°C. Figure 1 presents a nomogram that can be used to determine t_{43}.

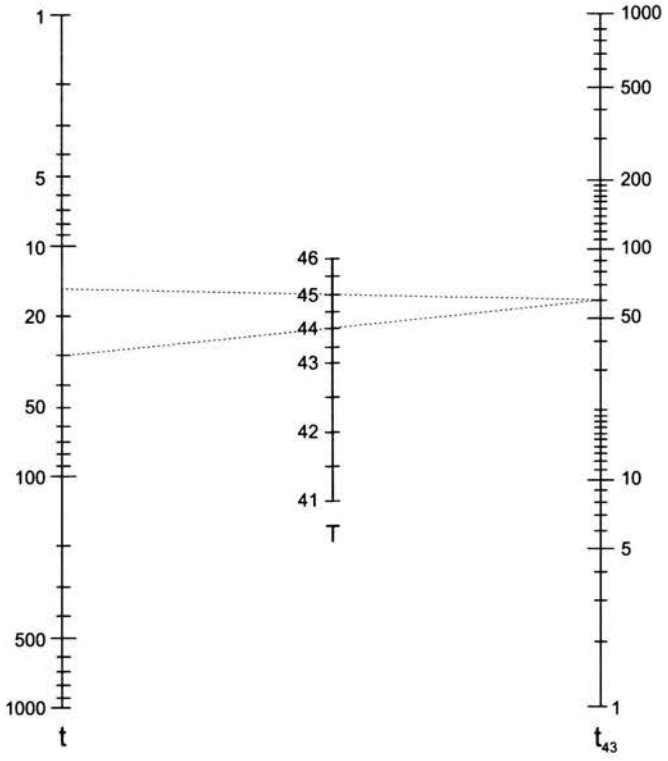

FIGURE 1. Nomogram that can be used to calculate t_{43} – equivalent time at 43°C, given the duration and temperature of the treatment. Example shows that the 15-min treatment at 45°C and 30-min treatment at 44°C are equivalent in the sense of this criterion, after [50].

The short duration and high intensity heat loads pertinent to orthopaedics are usually encountered during operation or therapy: during drilling or sawing of the bone, during the bone cement polymerisation within the bone and during hyperthermic cancer therapy. Conversely, small, long-term (usually cyclic) elevation of bone temperature is encountered postoperatively – during the functioning of the artificial joint. In the first case the detrimental consequences of the heating manifest after a short period of time – the bone cells die and are replaced by the fibrous bone tissue. This may lead to instability of the fixation and loosening. In case of the thermal treatment of the bone, dying of the bone cells is the desired effect, cf. [60].

In the present paper we concentrate on these two classes of thermal problems, i.e. short duration–high intensity heat loads and prolonged exposure to slightly elevated temperature. Main features of these problems are outlined in Table 1. We focus attention on the problems of exothermal bone cement polymerisation in the vicinity of the bone, heat generation during bone cutting and during joint articulation. Another class of problems related to the influence of high temperature on hard tissue is related to various hyperthermic treatments of bony sarcoma or adjacent soft tissues. Laser techniques used in periodontology, in the treatment of oral diseases, are a good example, cf. [55].

TABLE 1. Two types of problems in orthopaedic heat transfer.

heat load	**short duration, high temperature**	**long duration, moderate temperature**
area of application	bone cement polymerisation, bone drilling and sawing, hyperthermic treatments	artificial joint articulation
location	cement-bone interface, cut/drilled surface, site of the hyperthermic treatment (i.e. virtually anywhere)	articulating surfaces of the joint
other phenomena affected	kinetics of the bone cement polymerisation, thermal bone necrosis, aseptic loosening of the prosthesis, surgical trauma	acetabular cup wear and material degradation, diffusion of wear particles, aseptic loosening of the prosthesis
accompanying biomaterials	bone cement, metals	metals, UHMWPE, ceramics
max. temperatures	cement polymerisation: up to approx. 60°C at the bone surface and over 100°C within cement domain (dependent on the type of cement); sawing: over 150°C (sawing without coolant)	around 43°C in the middle of the prosthesis head and less than 40°C on the surface of bone

The freezing and lyophilisation of the bone fragments before the storage and implantation in the case of heterogenous bone implants is out of scope of these notes, since essentially no living tissue is involved in these techniques.

In the outlined investigations of the thermal problems various experimental techniques, *in vitro* as well as *in vivo* are usually used. Also biomaterials (i.e. the materials, produced by man and used for settlement in the living organism in the role of implant, fixation or substitution) undergo experimental testing to determine their various thermal properties.

From the physical point of view, the solution of the problems characterized in Table 1 consists of finding the transient temperature distribution in highly heterogenous tissue domain subject to heat fluxes of various origin. The practical information to be obtained is usually the value of the highest temperature within the living tissue and the duration of the heating. Additional analysis can provide the degree and extent of the thermal damage, deterioration of the mechanical properties (e.g. creep of the polyethylene acetabular cups, microcracking of the bone cement mantle), possible chemical damage (e.g. by the bone cement radicals) etc.

We now proceed to examination of the modelling techniques used in the case of polymerisation of bone cement. The hip endoprosthesis setup will serve as an example.

2. Heat generation during bone cement polymerisation – hip endoprosthesis

The prosthesis setup is sketched in Fig. 2 (intramedullary component of cemented hip prosthesis) and in Fig. 3 (cemented acetabular part). The stem of the endoprosthesis is cemented in the medullar cavity of the femur with the polymethylomethacrylate (PMMA) bone cement which is inserted by the surgeon in a "doughty" state and then polymerises in situ. The acetabular cup can also be fixed in the pelvis with the use of cement. Cemented implants are also used in the case of the knee joint reconstruction, cf. [46, 47]. The polymethylomethacrylate bone cement is also often used for filling the voids in bone and for fixation of other joints than hip joints (acromioclavicular joint, elbow joint etc.). Mercuri [36] provides a description of the use of PMMA in stabilisation of fossa component of temporomandibular joint prosthesis.

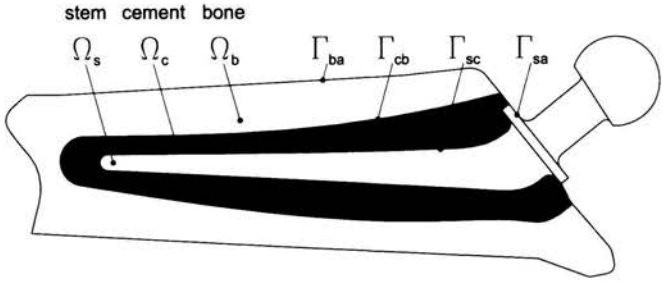

FIGURE 2. Intramedullary cemented part of femoral prosthesis, the domains distinguished in further analysis are labelled with Ω, domain boundaries are labelled with Γ supplemented with obvious subscripts.

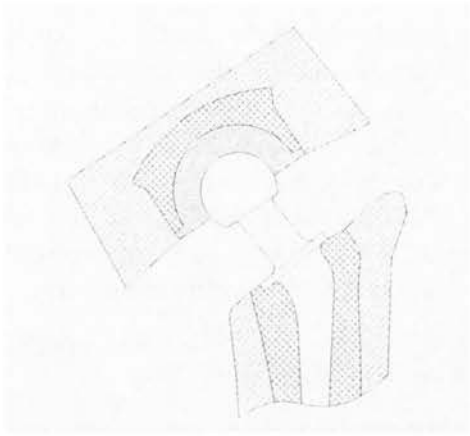

FIGURE 3. Cemented acetabular part of femoral prosthesis.

The popularity of cemented implants originates from the fact that the undesired effect of 'stress-shielding' is reduced in such a setup, when compared to cementless ones. Stiffness of the cement mantle is intermediate between that of the metal prosthesis stem and that of the bone. The statistical data to support this view can be found in [43] and [65]. Prostheses inserted in say knee and hip joints of rheumatoid patients are usually cemented ones.

Due to the implantation of the cemented prosthesis several dangers may arise. Here, we concentrate on those associated with thermal problems. The exothermal polymerisation of the bone cement in-situ can be the cause of:

- *Thermal bone necrosis* – the elevated temperature at the site of the implantation is applied directly to the bone. In consequence, bone resorption may occur, leading to aseptic loosening [35, 44, 69]. It is now generally believed, that the development of modern 'low-temperature' cements has reduced this danger considerably.
- *Chemical damage to bone* – some researchers support the view, that the free radicals, present at the early stages of the polymerisation along with the leftover monomer substantially contribute to the bone necrosis [32, 69]. It is noteworthy that it is not a generally accepted view. Some scientists argue, that the surgical trauma caused by the process of the preparation of the implantation site prior to cementing has much more detrimental effect than the toxical chemical agents released from the cement dough, see [32].
- *Pre-cracking of the cement mantle* – large elevations and substantial gradients of the temperature during the polymerisation are supposed to cause a high level of stress and consequently damage of the cement

mantle. This hypothesis is supported by the experimental and numerical findings of Lennon and Prendergast [30].

Thus the analysis of the temperature distribution in the implant system during and after polymerisation would allow the assessment of the thermal and chemical dangers to the living tissue as well as the assessment of the mechanical dangers to the load-bearing cement mantle. It is also worth noting that physical properties of the cement are most probably dependent on the history of polymerisation and hence on the temperature history.

2.1. Experimental methods

The relevant experimental contributions available can be divided into the following categories:

- measurements of the thermal properties of biomaterials used in arthroplasty (including identification of the polymerisation kinetics), cf. [1, 35],
- measurements of the thermal properties of the bone tissue *in-vitro*, cf. [6],
- measurements of the temperature rise in the implant system *in vivo*, cf. [45, 51, 62, 72],
- measurements of the temperature rise in the simulated implant system, cf. [15, 25, 36],
- long-term experiments on animals and follow-ups of the human cases designed to determine the effect of the arthroplasty on the bone, cf. [51, 69].

For the identification of the polymerisation kinetics the researchers nowadays usually choose *Differential Scanning Calorimetry* in the isothermal regime, cf. [1, 35] and the references therein.

In vivo and *in vitro* temperature measurements of hip joint have also been performed by researchers working on frictional heat generation and these experiments, see [3, 4].

An extensive follow-up study of 28 human total hip arthroplasty cases was performed by Wilert et al. [69]. The specimens were obtained by means of biopsy during the reoperation and during the autopsy – from patients that died from reasons unconnected with hip problems. The samples taken at various times after the implantation were prepared and the observations of the bone–cement interface were made with the use of microscope. The main conclusion of their work can be summarized as follows: in the specimens taken at no more than three weeks postoperatively a wide zone of necrosis (3 mm) was observed in the implant bed. This was attributed mainly to the thermal

effect of the polymerising cement. There were also some infarct-like areas of necrosis at some distance from the cement, caused probably by the vascular disruption during the operation. Active repair and remodelling continued for one year or longer. Necrotic bone was remodelled, reinforced or replaced.

The permanent implant bed showed a thin connective-tissue membrane surrounding the cement. The bone remodelling continued at minimum rate. For detailed, instructive observations and conclusions the reader is referred to [69].

2.2. Modelling

When modelling the heat transfer in the cemented bone–implant system the following simplifications are usually imposed:

1. Axial symmetry of the model along the axis of the stem, see [35, 56, 58]. In [22] a two–dimensional, axisymmetric model was considered.
2. Perfect thermal contact between the materials [58]. In [35] several areas of null contact are considered on an otherwise perfect thermal interface; in [22] and in [56] nonzero thermal contact resistance was allowed.
3. Temperature-independent material moduli, see [22, 35, 56, 58].
4. Material isotropy, [22, 35, 56, 58]. This assumption can be easily generalized but the lack of reliable material coefficients is the major obstacle. There are a few experimental measurements of anisotropic thermal properties of the tissue and these usually do not encompass all the components of the thermal conductivity (or diffusivity) tensor, cf. [13] and [41].
5. Constant boundary conditions, independent of temperature, see [22, 35, 56, 58]. The temperature in a biological system is thus assumed to vary over a range small enough to allow for changes in the boundary convection to be disregarded. Otherwise the convection coefficient should be reiterated for every computed boundary temperature. In view of the relatively small temperature variation, this should be regarded as a reasonable assumption.
6. Excluding the surrounding muscle tissue from the model, see [22, 35, 56, 58]. Modelling the soft tissue presents difficulties since the effect of vascularity must be accounted for. It can be done in a simple way by adopting one of the known continuous bio-heat models, e.g. Pennes equation, Weinbaum-Jiji equation, hybrid models, etc., cf. [42, 67, 75]. Other possibility is to construct *a vascular model* accounting for the exact architecture of blood vessels in the limb. For a review of modelling of the heat transfer in soft tissues see [57].

Various simplifications are also often introduced at the stage of modelling of the thermal effect of bone cement polymerisation, i.e. PMMA polymerisation kinetics.

Simplifications listed above originate mainly from the lack of knowledge that would be required to construct more sophisticated models. For example, the thermal conductivity of the bone tissue as reported in numerous papers on the subject (see e.g. [6, 10, 22, 35]) varies from 0.26 to 0.60 $\frac{W}{mK}$ and the specific heat varies from 1150 to 2370 $\frac{J}{kgK}$, etc. These measurements were performed on fresh and on the dry human cadaveric femur. For detailed report from measurements of variation of thermal properties along femur the reader is referred to the work of Biyikli et al. [6].

Generally, the bone tissue material parameters depend on multiple factors, mainly the bone composition (cortical/spongeous) and bone marrow and water content. These properties vary along the bone and are different for different individuals.

2.2.1. Formulation of the heat transfer problem The unknown function is the temperature T in the domain Ω. In the models, that exclude surrounding soft tissue, Ω is essentially reduced to the sum of geometrical domains of prosthesis stem, cement and bone domains, when intramedullar part is considered, or prosthesis head, acetabular cup, cement and pelvis fragment domains, when acetabular part is studied. In many cases considering the heat exchange in the surrounding layer of muscles is also necessary.

The starting point in construction of a mathematical model is the energy balance equation, cf. [7, 70],

$$\rho c \frac{\partial T}{\partial t} + \nabla \mathbf{q} = q_v, \tag{2.1}$$

where t denotes time, $\mathbf{q}$ is the heat flux vector, q_v is the volumetric heat generation rate, c and ρ denote the specific heat and density, respectively. Taking into an account the constitutive equation (Fourier's law):

$$\mathbf{q} = -\boldsymbol{\lambda} \nabla T, \tag{2.2}$$

we obtain the Fourier-Kirchhoff equation:

$$\rho c \frac{\partial T}{\partial t} = \nabla \cdot (\boldsymbol{\lambda} \nabla T) + q_v. \tag{2.3}$$

Equation (2.3) is satisfied separately in the stem, bone, cement and muscle domains (Ω_s, Ω_b, Ω_c, Ω_m):

$$\begin{cases} \rho_s c_s \dfrac{\partial T}{\partial t} = \nabla \cdot (\boldsymbol{\lambda_s} \nabla T), & \mathbf{x} \in \Omega_s, \\ \rho_b c_b \dfrac{\partial T}{\partial t} = \nabla \cdot (\boldsymbol{\lambda_b} \nabla T), & \mathbf{x} \in \Omega_b, \\ \rho_c c_c \dfrac{\partial T}{\partial t} = \nabla \cdot (\boldsymbol{\lambda_c} \nabla T) + q_v, & \mathbf{x} \in \Omega_c, \\ \rho_m c_m \dfrac{\partial T}{\partial t} = \mathcal{B}(\mathbf{x}, T, T_{,i}, T_{,ij}), & \mathbf{x} \in \Omega_m. \end{cases} \tag{2.4}$$

The subscripts s, b, c, m denote the prosthesis stem, bone, cement and soft tissue respectively. Since different bioheat equations can be used, the last equation is not stated explicitly in the above formulation and instead an operator $\mathcal{B}$ is used. For a review of available bio-heat equations the reader is referred to [57].

In the cement domain the nonzero heat generation rate q_v arises due to the non-adiabatic polymerisation process. One needs a model of the polymerisation process to calculate that rate. Apart from that, the modelling of polymerisation is undertaken for such purposes as:

1. to enable one to compute the thermal stresses in the cement mantle,
2. to predict chemical and physical outcome of the polymerisation process in cement domain, i.e. resulting properties of the cement mantle (monomer leftover, porosity etc.).

We note that the calculation of thermal stress receives recently an increasing attention, cf. [30, 31, 68].

Let us pass now to brief synthesis of available methods of modelling of PMMA polymerisation. To do it in a systematic manner we shall introduce the scalar variable called the *polymerisation fraction* describing the progress of the polymerisation process at a given material point. The polymerisation fraction is defined in terms of the released heat fraction [1]:

$$w(\mathbf{x}, t) = \frac{1}{Q_{\text{total}}} \int_0^t q_v(\mathbf{x}, t)\, dt, \tag{2.5}$$

where Q_{total} is the total heat of the polymerisation per unit volume and q denotes the local heat generation rate per unit volume. The above definition implies that at the time $t = 0$ the polymerisation fraction is zero.

One immediately notes the difficulties inherent in such a definition. Namely, to measure the total heat of polymerisation Q_{total} one needs to conduct an experiment, where polymerisation takes place and to measure the heat released. There is no guarantee, however, that the heat released is the *total heat of polymerisation* i.e. no more heat can be released if different polymerisation history (e.g. different temperature profile) is applied.

After the differentiation of Eq. (2.5) we see that the volumetric heat generation rate q_v is proportional to the rate of change of w, i.e. the polymerisation rate. This quantity is described by the kinetics equation of the form

$$\frac{\partial w}{\partial t} = f(w, T, t), \tag{2.6}$$

where f is a prescribed function. Spatial dependence is not included since initial material homogeneity is assumed.

Different ways to approach the problem of the PMMA polymerisation coupled with heat transfer within cement will be now presented in the order of increasing complexity.

Instantaneous polymerisation

This model assumes instantaneous polymerisation over the whole cement volume with the release of the heat equal to Q_{total} per unit mass, which uniformly heats up the cement domain. Only calculation of the temperature field is possible and therefore such model can not predict the monomer leftover. The function f on the r.h.s. of Eq. (2.6) for such a model takes the form of the Dirac delta function of time only:

$$f(w, T, t) = \delta(t).$$

Therefore modelling the heat generation in the cement is equivalent to imposing the appropriate initial condition:

$$T(\mathbf{x}) = \begin{cases} T_0 & \text{if } \mathbf{x} \in \Omega_s, \\ T_{\text{body}} & \text{if } \mathbf{x} \in \Omega_b, \\ T_0 + \dfrac{Q_{\text{total}}}{c_c} & \text{if } \mathbf{x} \in \Omega_c, \end{cases} \tag{2.7}$$

where T_0 denotes the ambient temperature, T_{body} is the normal body temperature and c_c is the specific heat of the cement. Then the transient equation of heat conduction is solved to obtain the maximum temperature rise on the bone domain boundary. Such a model of the acetabular implant was constructed and solved by Jefferiss et al. [25] for the one-dimensional case.

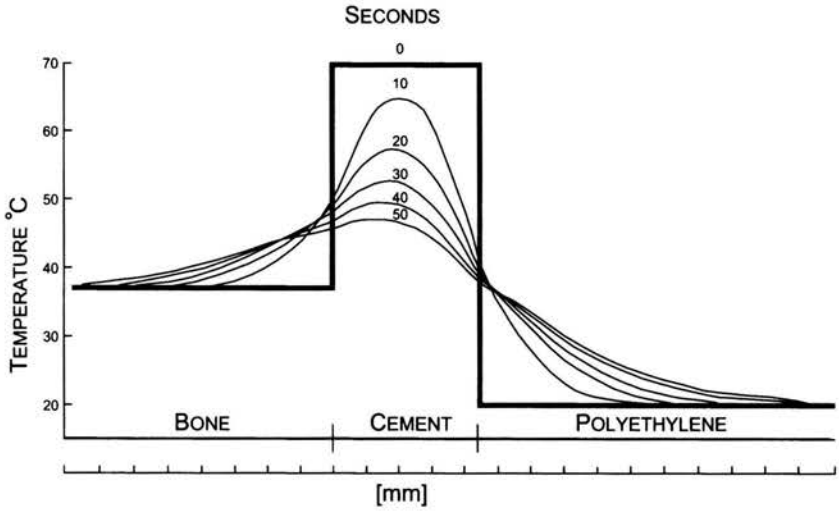

FIGURE 4. Temperature field relaxation in the one-dimensional model of cemented implant with instantaneous polymerisation. Thick line denotes discontinuous initial condition, after [25].

Figure 4 presents the results. Discontinuous initial condition (2.7) is distinguished with the thick line. As can be inferred from Fig. 4 the initial temperature of 70°C produces temperatures of the order of 50°C at the bone-cement interface in the first stage of the process of heat dissipation. Jefferis et al. [25] argue that the instantaneous polymerisation model will always yield higher tissue temperatures than any other model, where the energy is released over the finite time period. Therefore the data presented in [25] are supposed always to reflect the "worst case" in terms of tissue damage. It should be observed, however, that this would only be the case if the tissue-damage criterion was based on the temperature only, not on the temperature history. The experimental data suggest that preheating lowers the ability of the tissue to withstand elevated temperatures. Therefore such simplified model of heat release during polymerisation might not be satisfactory.

Uniform, time-dependent polymerisation

In this model the polymerisation extends over the finite period of time and the heat generation rate function is assumed to have a prescribed form (obtained from the experiment). The function f on the r.h.s. of Eq. (2.6) is dependent neither on the temperature nor on the current polymerisation fraction and is thus given by

$$f(w,T,t) = p(t).$$

The heat generation rate is therefore uniform. The temperature field during polymerisation needs not to be uniform. This model gives also no information about the distribution of final monomer leftover but an attempt is undertaken to make the model resemble the real situation more closely. The properties of cement such as the retardation time can be modelled here. Still only a linear equation of heat conduction needs to be solved.

The function $p(t)$ is assumed to satisfy the requirement $\int_0^\infty p(t)\,dt = 1$ and apart from that is arbitrary (its shape is based on experimental data). Such an approach was used by Huiskes [22] and by Swenson et al. [58]. Figure 5 presents various polymerisation functions, i.e. integrals of $p(t)$, used in [22]. The rate of these functions determines the heat generation rate at any moment in time. It has been found that the choice of the polymerisation rate function affected mainly the temperature history, whereas the change in peak temperature was very small.

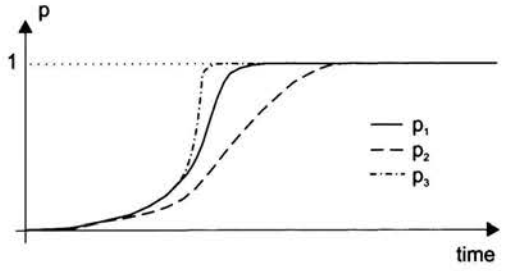

FIGURE 5. Three polymerisation functions used by Huiskes [22].

The model of the instantaneous polymerisation can be viewed as a specific case of the more general, time-dependent polymerisation model but its greater simplicity justifies distinguishing it as a separate case.

Temperature-dependent polymerisation without monomer leftover

Such models describe the fact that the polymerisation rate is dependent on the temperature and the instantaneous polymerisation fraction. Explicit time dependence is neglected and the function f on the r.h.s. of Eq. (2.6) has the form

$$f(w,T,t) = u(w,T). \tag{2.8}$$

It is convenient to describe this function in a factorized form

$$u(w,T) = A(T)P(w). \tag{2.9}$$

The function P can be identified from experiments in the isothermal regime, while A is a temperature-dependent scaling factor. The function $P(w)$ must

satisfy the requirement $P(1) = 0$ and $P(w) > 0$ since polymerisation is an irreversible process. Many experimental data indicate that also $P(0) = 0$ must hold; see [1] and the references cited therein. Baliga et al. [1] proposed the following form of the function $P(w)$

$$P(w) = w^{\beta}(1-w)^{\gamma}, \tag{2.10}$$

where β and γ are constants independent of temperature.

The temperature-dependent scaling factor was obtained by means of curve-fitting and was computed by Baliga et al. [1] on the basis of earlier experiments:

$$A(T) = 10^3 \times \left(-105116 + 13056\,T - 595.307\,T^2 + 12.736944\,T^2 + \right.$$
$$\left. -0.12349128T^4 + 4.443296 \times 10^{-4}\,T^5\right), \tag{2.11}$$

where T is expressed in °C. In shape, the measured $P(w)$–curves resembled 'skewed parabolas' but the magnitude of these discrepancies was found negligible, cf. [1], hence the constants α and β were assumed equal to unity.

While freedom of choice of mathematical formulae to describe experimental data is unquestionable, the chemical process underlying the polymerisation is hardly expected to follow fifth order polynomial law. For this reason this model should be considered as tentative. One can propose an exponential description, such as in the subsequent model.

Temperature-dependent polymerisation with monomer leftover

This model uses multiplicative decomposition of the polymerisation rate function as presented in Eq. (2.9). In this model the assumption $P(1) = 0$ is replaced by its more general form $P(w^*) = 0$ while the remaining assumptions are unchanged. The quantity $0 \leq 1 - w^* \leq 1$ is temperature-dependent equilibrium monomer leftover, in general not equal to zero. One notes that both terms of the r.h.s. of Eq. (2.9) become dependent on temperature but the factorized form is retained for clarity.

Mazzullo et al. [35] proposed the bilinear variation of the function w^* with absolute temperature:

$$w^*(T) = \begin{cases} \dfrac{T}{T_g}, & \text{if } T \leq T_g, \\ 1, & \text{if } T > T_g, \end{cases} \tag{2.12}$$

where T_g is the *glass transition temperature.*

Consequently, the function P takes the form, see Eq. (2.10),

$$P(T,w) = \begin{cases} \dfrac{\alpha}{w^*(T)} w^{1-1/\alpha} \left(w^*(T) - w\right)^{1+1/\alpha}, & \text{if } w < w^*(T), \\ 0, & \text{if } w \geq w^*(T). \end{cases} \tag{2.13}$$

In comparison with the previous model the two independent exponents β and γ are expressed by a single constant α where $|\alpha| > 1$. In Fig. 6 the form of the function $\frac{P(w,\alpha)}{\alpha}$ is depicted; we assume $w^* = 1$.

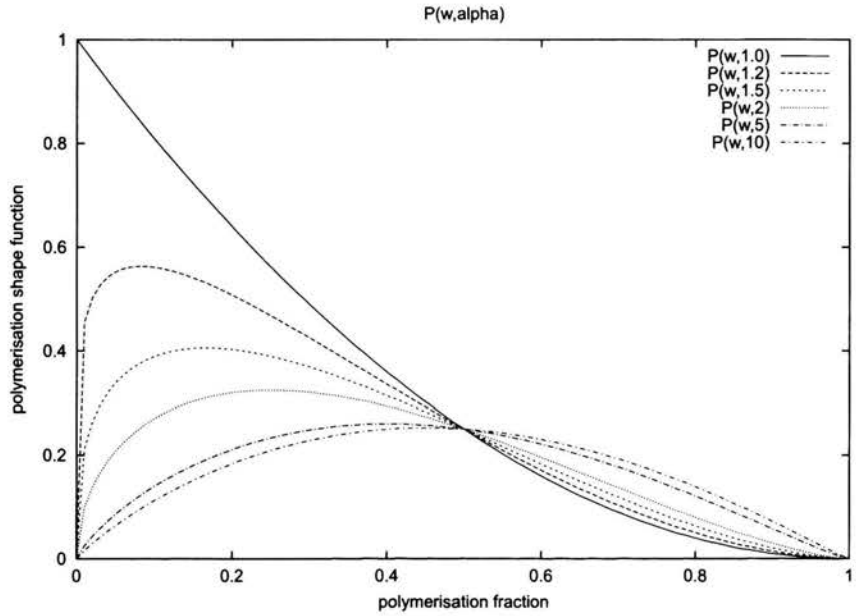

FIGURE 6. Function $P(w,\alpha)/\alpha$ as proposed in [35]; w^* is assumed equal to one here and the multiplicative term α is dropped for clarity.

Mazzullo et al. [35] experimentally obtained $\alpha = 9,2$ (Howmedica Simplex-P cement). As can be seen in Fig. 6 the deviation from the parabolic form is minimal.

The temperature-dependent scaling factor used by Mazzullo et. al [35] takes the form of the Arrhenius-type relation:

$$A(T) = a \exp\left(-\frac{E_a}{RT}\right). \tag{2.14}$$

It should be noted that the form of the function $A(T)$ in Eq. (2.14) is very similar to the one obtained experimentally by Baliga et al. [1] and presented

in Eq. (2.11). The constant E_a has a physical meaning of the energy of activation, R is the universal gas constant and a is the frequency constant. The values of the constants of the model are collected in Table 2. In Fig. 7 the polymerisation rates for different temperatures are depicted. It is worth noting that the end point of the process drifts to the right with increasing temperature. Also a fixed increase in the temperature of the process results always in the same shift of this end point provided that $w_{end} \neq 1$. This is a straightforward consequence of Eq. (2.12).

TABLE 2. Polymerisation constants used in Eqs. (2.12)–(2.14), after Mazzullo et al. [35].

$Q\ [\frac{\text{J}}{\text{kg}}]$	$a\ [\frac{1}{\text{s}}]$	$E_a\ [\frac{\text{J}}{\text{mol}}]$	α	T_g [K]	$B\ [\frac{\text{J}}{\text{mol K}}]$
193.0×10^3	2.6397×10^8	62866.0	9.2	378.0	8.3143

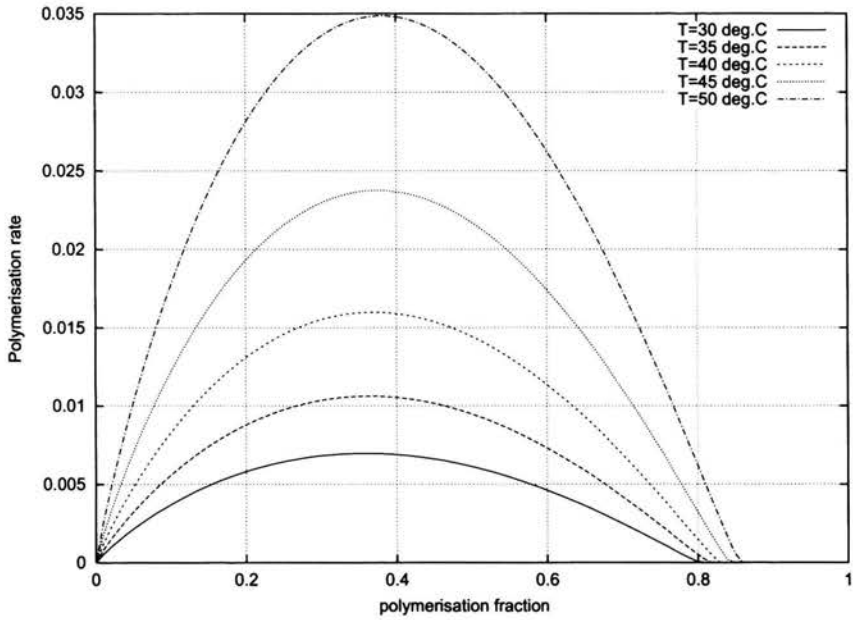

FIGURE 7. Polymerization rate versus polymerisation ratio for different temperatures (isothermal process). Model of temperature-dependent polymerisation with monomer leftover, after [35].

The polymerisation models presented are of phenomenological nature. While constants for the models presented here correspond to commercially available surgical cements, the actual behaviour of the cement is also depen-

dent on its chemical composition. For some results on this topic the reader is referred to [9].

Now, the boundary conditions need to be specified. The boundary of the considered domain is denoted

$$\Gamma = \partial(\bar{\Omega}_s \cup \bar{\Omega}_c \cup \bar{\Omega}_b \cup \bar{\Omega}_m),$$

where the bar denotes the closure of the domain. Only the Fourier boundary condition (corresponding to the Newton law) is considered:

$$\lambda \frac{\partial T}{\partial \mathbf{n}} = \alpha(T_f - T), \qquad \mathbf{x} \in \Gamma. \tag{2.15}$$

Here T_f and α are prescribed functions on the boundary Γ, representing ambient temperature and convection coefficient, respectively.

To complete the formulation of the problem thermal contact conditions have to be specified. These are the continuity of the heat fluxes across the contact surfaces. The temperature might be discontinuous across these surfaces with the jump proportional to the normal heat flux across the interface. The interfaces are denoted by $\Gamma_{bc} = \bar{\Omega}_b \cap \bar{\Omega}_c$ (the interface between bone and cement domains), $\Gamma_{cs} = \bar{\Omega}_c \cap \bar{\Omega}_s$ (the interface between cement and stem domains). The constitutive equation on the bone–cement interface is given by:

$$\lambda_b \frac{\partial T_b}{\partial \mathbf{n}_b} = -\lambda_c \frac{\partial T_c}{\partial \mathbf{n}_c} = \beta_{bc}[\![T]\!], \qquad \mathbf{x} \in \Gamma_{bc}. \tag{2.16}$$

As usual $[\![f]\!]$ denotes the jump of f; $\mathbf{n}_b$ and $\mathbf{n}_c$ are outer normal vectors of the boundaries of the bone and cement domains, respectively. Assuming perfect contact between the bone and the cement means that $\beta_{bc} \to \infty$, i.e. that temperature jump across the interface must be equal to zero and nonzero heat flux across the interface can nevertheless be maintained.

In Table 3 the values of the material coefficients collected from the literature are provided after [4, 6, 10, 22, 35, 58] and [73]. It should be noted that these values correspond to a certain type of prosthesis considered here (metal stem, polyethylene (PE) distal plug, cf. [35]). As is well-known, there

TABLE 3. Values of material coefficients.

		stem	bone	cement	PE
conductivity	$\lambda \left[\frac{\mathrm{W}}{\mathrm{m\,K}}\right]$	14	0.26–0.60	0.17–0.21	0.29–0.45
specific heat	$c \left[\frac{\mathrm{J}}{\mathrm{kg\,K}}\right]$	460	1260–2370	1460–1700	2220
density	$\rho \left[\frac{\mathrm{kg}}{\mathrm{m}^3}\right]$	7800	1000–2900	1100	960

is a wide variety of materials used for prosthetic heads, acetabula, stems etc. whose properties may be different from the ones listed in Table 3.

In Table 4 possible values of interface conductivities are provided, cf. [22, 35]. The values for the thermal contact conductivity between polyethylene acetabular cup and cement and articulating surface of prosthesis head were estimated by Huiskes [22] to be of the order of $500\frac{W}{m^2K}$. One may suspect higher value at the latter interface due to the presence of the synovial fluid. In [56] different values of the thermal contact conductivity β were used, namely in the range $10^2 - 10^6 \frac{W}{m^2K}$ and the study revealed no significant change in the process when the values exceeding $\beta = 2000\frac{\mathrm{W}}{\mathrm{m^2K}}$ were used. So, according to the estimations provided in Table 4, the determination of the value of the thermal contact conductivity of the bone–cement interface may prove important. Since experimental data on this topic are scarce (see [17] for a review of recent developments) such research would be very helpful. The thermal contact conductivity is expected to depend on contact pressure and the kind of surface (polished/cleaned vs. rough/contaminated).

TABLE 4. Values of the interface conductivities/convection film coefficients, the values are in $[\frac{\mathrm{W}}{\mathrm{m^2K}}]$, after [22].

	cement	**ambient**
metal stem	1000–10000	50–100
bone	100–1000	500–10000

The values of the interface conductivities have a significant influence on both the temperature distribution and on the monomer leftover. In Fig. 8 the simulated dependence between the thermal conductivity and the overall volume-averaged final degree of polymerisation is presented. Details of the numerically simulated model are given in [56].

We have not discussed here the modelling of the heat transfer in soft tissue layer. A variety of such models is available, cf. [57]. Including them in a a complete formulation is an important step in constructing the mathematical model of heat exchange in human limb or extremity, cf. [53, 71, 74].

The purpose of calculation of temperature/monomer leftover distribution throughout the cement mantle is to assess the quality of the chosen prosthesis fixation technique, to estimate danger to the living tissue and to predict the probability of possible loosening of the prosthesis as an effect of resulting damage. To this end one needs criteria of thermal/chemical damage to the bone tissue (bone necrosis) that one can compare with computed values of the temperature and monomer leftover.

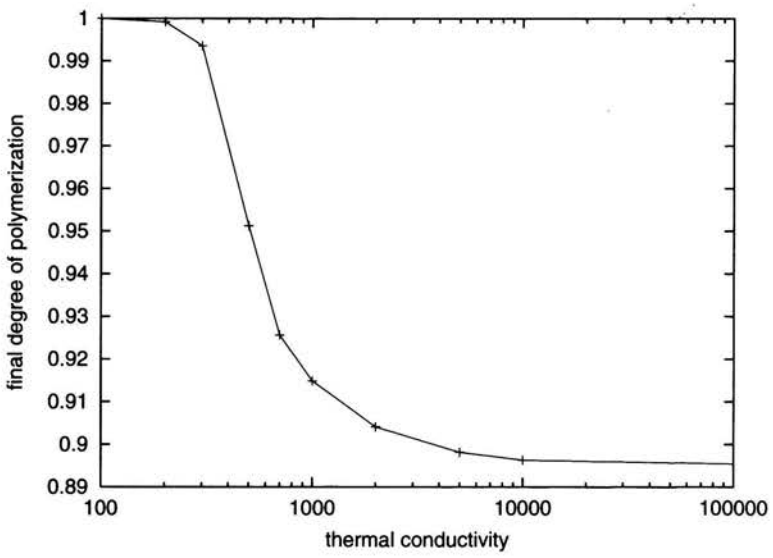

FIGURE 8. Volume-averaged final polymerisation ratio dependence on the thermal contact conductivity $[\frac{W}{m^2K}]$ taken uniform and the same for all the interfaces. Details of the model are given in [56].

In general, the use of polymethylomethacrylate (PMMA) bone cement in the orthopaedic surgery may lead to threats. Theses can be classified as follows, cf. [18, 25],

1. vascular disturbance at the site of implantation,
2. disruption of the cortical and marrow circulation,
3. thermal necrosis during polymerisation,
4. chemical necrosis during and after polymerisation,
5. introduction of residual stresses (thermal stresses) to the cement mantle.

We consider here only points 3 and 5, although the formulations presented encompass also the phenomena of incomplete polymerisation and allow, in principle, to predict chemical damage to the tissue. For the experimental investigation of chemical trauma the reader is referred to Linder [32], where cement dough was implanted into rabbit tibia and care was taken to minimise the mechanical and thermal injury. The reported chemical trauma was very limited, giving rise to speculation that the primary injury mechanism during implantation is of mechanical nature, i.e. vascular injury, blocking of Haversian canals by cement or intramedullary fat particles during drilling, etc.

Presented models can form a basis for a thermomechanical analysis. Thermally-induced residual stress can potentially lead to crack growth in the cement and can cause debonding and prosthesis loosening. The significant factor is also the cement porosity which causes local stress concentrations. Kusy [27] distinguishes two kinds of porosity: intrinsic and acquired, the former being the result of cement curing whereas the latter results from leaking out of the water-soluble components of the cement (e.g. antibiotics) over the period of months or years. Thus the overall porosity of the cement depends on its composition.

One of the most important factors contributing to the level of residual stress is the fact, that stress-locking occurs in the cement at the highest temperature attained during the course of polymerisation. This phenomena was observed during simultaneous measurements of the strain and temperature in a polymerising cement block [68].

Lennon and Prendergast [30] performed experimental investigations of the model of the cement mantle and appropriate numerical analysis using the polymerisation model due to Baliga et. al. [1]. The main finding is that cracks induced in the cement mantle during polymerisation are often perpendicular to the computed principal directions of stress. This supports the view that thermal stress induced by the heat of the polymerisation may significantly affect the fatigue life and mechanical properties of the cement mantle.

Nuño and Avanzolini [39] performed a numerical analysis of cemented implant system to determine whether potential residual stresses at the cement-stem interface changes the stress distribution that arises in response to external loads. Commercial FEM package ANSYS 5.4 was used. The residual stresses were prescribed, basing on the earlier experimental and numerical evidence. No polymerisation simulation was performed and the bone-cement interface was assumed fully bonded while, conversely, the stem-cement interface was assumed fully debonded (no adhesion) with press-fit. Details of the numerical simulation are given in [39]. The results showed a significant increase of the stress resulting from loading typical for the implant system due to the residual stress at the stem-cement interface. It should be noted, however, that the analysis was purely mechanical and the residual stresses were introduced by means of the press-fit, not by the thermal effects.

The issue of thermal bone necrosis has been investigated by many researchers. The results suggest two basic mechanisms. One is the collagen protein denaturation. According to Swenson et al. [58], it takes place at temperature range 56–70°C. The second mechanism is caused by cellular death, which occurs at lower temperatures and is therefore more important. The results presented in [4, 3, 5, 22, 35, 58] and [60] point out the time–temperature dependence inherent in thermal necrosis criteria. For example, the tempera-

ture of 70°C is believed to kill cells instantly, 50°C needs to be maintained for 30 seconds and 45°C – for 5 hours. Higher temperatures (of order 70°C) are needed to destroy the regenerative capacity of the bone tissue, cf. [22, 58].

From the available data a straightforward mathematical criteria, based on the 'additivity rule' has been constructed by Mazzullo et al. [35]. Assume the time necessary to cause thermal bone necrosis at a given temperature T to be given by

$$t_c = M \exp\left(\frac{\mu}{R(T - T_{\text{ref}})}\right), \qquad T > T_{\text{ref}}. \tag{2.17}$$

Obviously, as $T \to T_{\text{ref}}$ time to necrosis t_c becomes infinite and below the reference temperature T_{ref} no thermal damage processes take place. M and μ are model constants. In prescribed non–isothermal conditions the local measure of thermal bone tissue damage η can be constructed as an integral of fractions of exposure time at given temperatures over time

$$\eta(\mathbf{x}, t) = \int_0^t \frac{dt}{t_c\big(T(\mathbf{x}, t)\big)}. \tag{2.18}$$

The values of η equal to or in excess of unity indicate local bone necrosis. This criterion is analogous to Palmgren-Miner hypothesis of linear damage accumulation in fatigue mechanics and has similar drawbacks. For example, it does not take into account the succession of the different stages of thermal load; thus various intensity heating periods will produce the same 'damage', irrespective of their relative order.

The necessary constants for the model were obtained by Mazzullo et al. in [35] by means of linear regression analysis and are given in Table 5. The criteria just described are similar to Miner hypothesis of linear damage accumulation used to describe fatigue of materials under varying cycle loading.

TABLE 5. Experimental constants for thermal bone necrosis criteria appearing in Eq. (2.17), after Mazzullo et al. [35].

M [s]	μ $\left[\frac{\text{J}}{\text{mol}}\right]$	T_{ref} [K]
1/27.4	1000.0	310.0

While it seems to be a good measure for a single heat shock cellular damage, this criterion may be insufficient when dealing with repeated thermal bone loading as the living tissue can probably adapt to higher temperatures by means of producing 'heat shock' proteins. It is not known whether they also exist in normal human joint, but this is feasible as natural joints heat

up by ca 2.5°C during walking and probably more during more intensive activities, cf. [61].

Reckling and Dillon [45] concluded their measurements of temperature at the bone-cement interface in acetabular component with the statement that temperatures high enough to cause bone necrosis are not attained during the polymerisation of the cement. Conversely, Schatzker et al. [18] measured temperatures of order of 75-95°C at the bone-cement interface *in-vivo*. This value is high enough to cause thermal bone necrosis.

The toxic leftovers of the polymerisation process are considered to be a more challenging problem. The negative influence of residual monomer, which is a powerful fat solvent and free radicals released from the cement dough is substantially prolonged when compared with pure high–temperature damage. Wilert et al. cit. by Swenson et al. [58] reports 3 mm necrotic zone in 3–weeks postoperative specimens. Possible damage mechanisms were identified to be PMMA polymerisation heat, free radical release and vascular damage. Goodman et al. [18] investigated the influence of acrylic cement on proximal humeral and proximal tibial methaphysis of the dog in the minimally loaded state. The animals were killed at 2, 4 and 5 months after the operation and the histological sections were done. Apart from other observations made by Goodman et al. [18] it is worth noting that the small quantities of the cement were found in the marrow spaces and in the Haversian canals indicating finger-like penetration outside the cement domain. The cement plugging of the Haversian canals resulted in localized areas of necrosis. Measurements of the remodelling activity were also made and the periprosthetic bone was significantly less active. The study presented in [17] suggests that after implantation into the site characterized by low level of mechanical loading the cement is encapsulated by thin connective tissue membrane containing scattered histiocytes and giant cells. Inflammatory cells were seldom observed. Unlike in the case of weight-bearing implants the synovial-like fluid and fibrocartilage were absent. Although marrow necrosis did occur in areas surrounding the cement implant, viable marrow has been found also in the nearest vicinity of the implant. This effect suggests that the blocking of Haversian canals and not, or at least not only, the toxic influence of monomer leftover is the factor that contributes to the bone tissue necrosis.

It seems therefore important to model the polymerisation process as well as temperature distribution and to develop criteria similar to (2.18) for assessing the tissue damage due to polymerisation leftover.

The eventual effect of bone necrosis is bone resorption at the bone–cement interface. The mantle of fibrous connective tissue is developed and the mechanical load–carrying capacity of the interface is seriously compromised, which usually leads to implant loosening and the need for reoperation.

Different measures are taken or considered to remedy this problem. These are:

1. implanting cementless prostheses,
2. development of new low–temperature and bioactive bone cements, cf. [49, 52, 66] and the discussion below,
3. water cooling (acetabular parts of total hip implants, cf. [72]),
4. shielding layers, cf. [22, 35],
5. lowering thermal contact between cement mantle and the bone which can also have a beneficial effect of lowering monomer leftover, cf. [56],
6. pre–cooling or pre–heating the prosthesis stem (possibly the bone and cement mixture),
7. using as little cement as possible.

The most straightforward method is to refrain from using cemented implants at all, in favor of cementless ones. There are, however, extensive clinical data from postoperative followups indicating that percentage of failures, marked by the necessity of revision, is significantly lower in the case of cemented prostheses, see [43] and the references cited therein. Also, cementless implants are avoided in the case of weaker bones, like in the rheumatoid patients.

The most promising method is to develop new cements that polymerise at low temperatures leaving no monomer leftover. Another advantage of lowering the maximum temperature in the system (not necessarily bone temperature) is that some heat-labile cement components (e.g. antibiotics) are not deactivated during the cement setting and also the potential problem of MMA boiling and cement porosity induced in this manner is avoided.

Lowering the peak temperatures during the polymerisation process reduces also the overall shrinkage of the cement during the cooling phase. As calculated by Holm [21] the final cooling of the cement is responsible for 40-50% of the final contraction (the coefficient of linear expansion is $\alpha = 2,27 \times 10^{-4}\ [\frac{1}{K}]$, see [21] and the references therein). It is well-known that the PMMA cement shrinkage is an undesirable effect that contributes to the loosening of the prosthesis.

The task of lowering polymerisation temperature can be in part accomplished by means of adding 'heat sink' additives to the PMMA powder and/or changing initial P/L ratio of cement mixture. Unfavourable outcome of these actions is the lower mechanical strength of the cement since its porosity increases. These issues are discussed in detail in [22].

Pre–cooling the prosthesis stem was proved to be ineffective cf. [5, 58, 62]; furthermore it was shown by Bishop et al. [5] that the low stem temperature

substantially deteriorates cement-stem interface quality and that pre-heating should be used instead of pre-cooling. Pre-cooling of the cement mixture also prolongs the setting period of the cement. In that period any motion of the installed prosthesis usually causes fixation failure. Implant has to be extracted from the femur, the cement has to be removed and new implant installed. Water cooling is possible only in acetabular components fixation and is reported to have a positive effect on the bone temperature [72].

The possibility of lowering the thermal contact between cement and bone was also investigated, cf. [22, 35]. Mazzullo et al. [35] showed that introducing thin layer of rubber-like material would have a beneficial effect on both the conversion of the monomer and temperatures of the bone. Such a barrier could also protect the tissue against the diffusion of toxic substances from the cement dough. Unfortunately, in view of the efforts to create the best possible environment for the bone tissue to grow into and 'interlock' with the cement such a solution should be considered impractical.

Another issue connected with the implantation of cemented prostheses that is worth mentioning is the fact that the mechanical properties of cement depend on the temperature. Therefore results of the tests conducted in the room temperature are not immediately applicable to the *in vivo* temperatures. Lee et al. [29] cited in [48] reported 4% decrease in the Young's modulus (in compression) and 10% drop in the ultimate compression strength at 37°C when compared to properties at room temperature. Lautenschlager and Marshall [28] measured the compressive strength of the plain Palacos-R cement at 0, 23 and 37°C and obtained the following values: 125.7 ± 1.8, 90.5 ± 1.1 and $86,9 \pm 2.5$ MPa. Jafee et al. [24] estimated the compression yield stress drop to be equal to 0.3 $\left[\frac{\text{MPa}}{^\circ\text{C}}\right]$. The work by Saha and Pal [48] contains a comprehensive review of the research on this topic. Also the work by Kusy [27] presents a comparison of chemical and physical properties of four commercially available bone cements.

3. Bone drilling and sawing during orthopaedic operations

As it has been outlined in Table 1, temperature increase during orthopaedic operations is of short duration but can be quite high. Two processes may lead to frictional bone heat-up during operation: sawing (e.g. during bone preparation for endoprosthesis implantation) and drilling (e.g. during preparation for screw fixation). The resulting thermal bone necrosis at the screw site leads to instability and consequently invalidates any benefits from any stabilising devices fixed to the bone. The correct choice of drilling/sawing parameters is therefore important. The parameters under consideration are:

- rate of rotation of the drill, speed of the saw,
- force on the drill or saw in the direction of drilling/sawing,
- the kind of tool, permitted level of wear,
- possible pre-drilling parameters,
- cooling(irrigation) parameters.

3.1. Experimental methods

The influence of above factors was measured experimentally, see [26, 34, 63]. The outcome can be summarized as follows:

- The rotational speed of the drill is reported to have no marked influence on the spatial temperature distribution in bone but it affects the duration of the exposure to high temperature – higher drill speeds produced high temperature for shorter periods [34]. Similar measurements made by Krause et al. [26] for high-speed (20,000 rpm and 100,000 rpm) cutting burs confirmed that that there is no general correlation between rotational speed of the bur and bone temperature, tendencies for different kinds of burs being different.
- The increase in force measured in the direction of drilling results in significant decrease of temperature in the vicinity of drill. Matthews

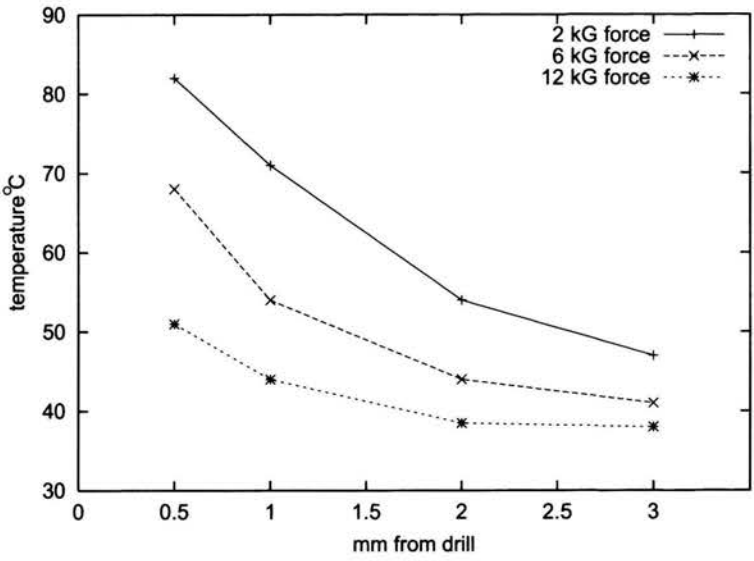

FIGURE 9. Temperatures recorded in bone for different axial forces during drilling, after [34].

and Hirsch [34] report approximately 15°C decrease (from ca 82°C) in location 0.5 mm from the drill when the force is changed from 2 to 6 kG and further 17°C decrease with force changed to 12 kG, see Fig. 9. Similar effect was reported by Krause et al. [26] for high-speed cutting burs; higher feed rates, and therefore cutting forces, cause lower temperature elevations. This tendency varied with kind of bur used. Effect of applied force magnitude is much more pronounced when duration of exposure to temperatures over 50°C is compared. For forces 2, 6 and 12 kG these durations are 35, 8 and ca 1 second respectively at the mentioned location.

In case of the dental burs and smooth pins used as drilling tools (as opposed to twist drills) the force is reported not to influence the temperatures in a way described above, Those tools have no means of eliminating the bone debris and therefore milling occurs rather than cutting and furthermore the debris gets compacted between the tool and the hole walls thus greatly increasing friction.

- Study of the influence of drill wear conducted in [34] showed that worn drills (used to drill 200 holes before) could produce temperatures over 20 K higher in the immediate neighborhood than new ones. Also time of exposure was significantly prolonged. As can be inferred from this one and other experimental investigations the shape of the tool has a marked influence on bone temperatures during drilling [26, 63]. The same applies to the saw, cf [64]. Figure 10 presents a comparison of temperatures measured by Krause et al. [26] for two different saw blades.
- The investigations of the effect of predrilling conducted by Matthews and Hirsch [34] showed temperatures during predrilling (drill diameter 2.2 mm) and subsequent enlarging of the hole (diameter 3.2 mm) to be virtually the same and, at the distance of 0.5 mm from the drill, ca 60 K lower than measured in control drilling (3,2 mm) (where temperatures exceeded 100°C). This result can be viewed as the proof of beneficial effect of predrilling or as the rough measurement of the influence of drill diameter on maximum temperatures attained, which turns out to be very high.
- Cooling of the drill and surrounding bone by means of irrigation with water is reported to lower the temperature of the bone substantially. Matthews and Hirsch [34] found that for their experimental setup and the diameter of drill they used (32 mm) no significant advantage was gained when raising the coolant flow above 500 ml/minute. The coolant they used was water at room temperature. Using pre-cooled water

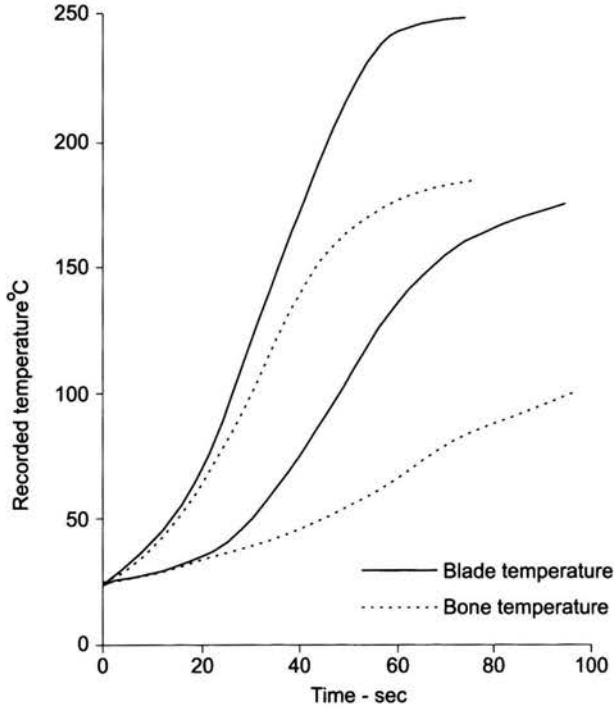

FIGURE 10. Recorded temperatures for two saw blades, after [26].

would probably allow less coolant to be used. The results of measurements conducted by Krause et al. [26] for different kinds of burs and reciprocating saws confirmed conclusion that cooling may significantly reduce the bone and tool temperature. Studies by Toksvig-Larsen et al. [63] with the prototype oscillating-blade saw showed that with adequate coolant flow the temperature elevations are negligible and well below the values usually associated with bone necrosis.

As can be seen from the above experimental results, appropriate choice of tools and cooling methods permits to avoid the danger of thermal bone damage during preparation for orthopaedic operation entirely.

3.2. Modelling

The problem of bone heating-up during sawing can mathematically be stated in the first approximation as finding the temperature distribution in the infinite solid with moving line heat source. The geometry is depicted

in Fig. 11. For steady conditions the solution is given in [7] by

$$T(x,z) = T_0 + \frac{q_l}{2\pi\lambda_b} \exp\left(\frac{Ux}{2a_b}\right) K_0\left(\frac{U\sqrt{x^2+z^2}}{2a_b}\right). \tag{3.1}$$

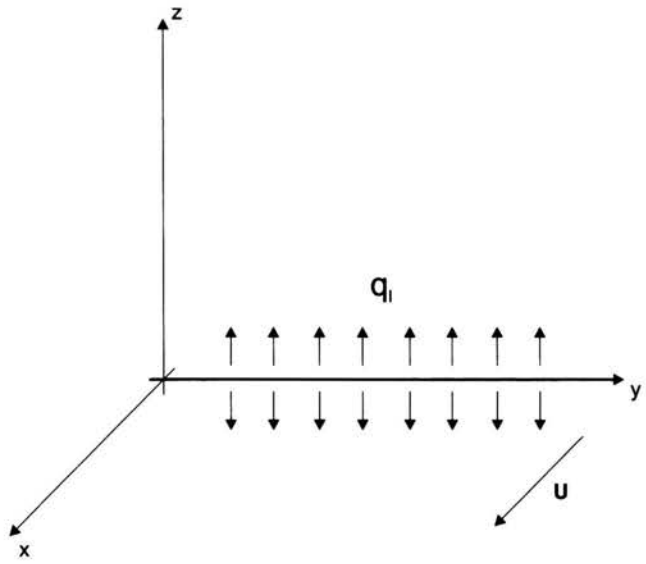

FIGURE 11. Idealisation of the problem of bone cutting: line heat source parallel to the y axis is embedded in the infinite medium moving in the direction parallel to x axis. The heat generation rate is q_l [W/m].

It is assumed here that infinite line source located at y-axis moves with the velocity U (sawing feed rate) in direction of x-axis. K_0 is the modified Bessel function of the second kind of order zero whilst λ_b and a_b are the thermal conductivity and thermal diffusivity of the bone respectively; q_l is the rate of heat generation expressed in $\left[\frac{W}{m}\right]$. The problem can also be visualized as the distribution of smoke in a medium, which flows past the line emitting smoke, cf. [7].

The closed-form solution (3.1) could be obtained due to the simplicity of the model. The assumptions not reflecting the physical situation are:

- Treating the bone specimen as an infinite solid. That assumption should result in under-estimating the temperatures as the heat is allowed to escape the real geometrical domain of the bone without any boundary resistance. This is thought to have no significant influence as long as the sawing process is fast.

- Treating the saw as a one-dimensional entity. This is reasonable for steady-state situations (deep cut), when the temperature of the saw does not change anymore. The heat flow through the blade in its direction and the blade heat capacity are thus neglected.

In such a formulation the crucial parameter q_l needs to be obtained experimentally by means of temperature or calorimetric measurements.

Alternatively to this formulation, Rosenthal (1946), cit. by Krause et al. [26], proposed a solution for an infinite solid with moving plane heat source instead of line source.

The problem of bone drilling could be analogously modelled by an infinite solid with moving point heat source. Again, the reported dependence of heat generated on feed rate (velocity U) is not predicted by the model and needs to be supplied. Furthermore, the diameter of the drill is also not a parameter, whereas experimental data strongly suggest its importance. Such a model should be therefore considered too simplified.

To summarise, we conclude that the problem of bone heat–up during drilling or sawing is nowadays not crucial since modern cutting tools are designed in such a way as to minimise or even completely eliminate the risk of thermal damage to tissue, cf. [63].

4. Frictional heat generation in joints

Friction occurs in all types of joints, both in natural and in artificial. The heat generation and dissipation is therefore a process that takes place every time the joint is used. In normal human hip joints the measured temperature elevation is of the order of $+2.5°C$ during walking and probably more during running, cf. [61].

The artificial joints are less efficient and one can expect that temperatures attained in such a joint can be higher. Bergmann et al. [2] reported a $3,5°C$ temperature increase in the case of titanium alloy hip prosthesis after 45 min. of normal walking. The temperature was measured inside the neck of the prosthesis. Its value at the bearing surface can be considerably higher, see [16, 33] for the finite elements estimation of this temperature for different articulating pairs: the zirconia, cobalt-chromium and alumina implant heads articulating on polyethylene cups.

Investigation of the problem of temperature distribution in an artificial joint, when the joint is being used is done for two specific reasons:

- To establish if thermal damage to the tissue can take place. Such a damage may lead to prosthesis, usually hip acetabular cup or knee prosthesis, loosening. The issue of criteria for thermal damage is more

difficult here than in the case of bone cutting or cement polymerisation because the thermal loading is now cyclic and this may result in 'thermal bone damage accumulation'. On the other hand it is suggested that bone tissue can develop 'heat shock' proteins and adapt to elevated temperatures, cf. [8, 37]. In fact, no adequate criterion is known to us.

- To assess the working temperatures and their influence on wear and creep rate of materials commonly used for articulating surfaces. In the case of polyethelene (PE, UHMWPE) implants the three most important factors contributing to failure are: excessive stress (which may be magnified by the presence of the residual stresses, cf. [40]), material oxidation due to γ–irradiation during sterilization and thermal damage. The latter is vital to long–term prosthesis performance. According to Young et al. [73] the Arrhenius–type relation can be applied to asses the time to failure t of polyethylene at elevated temperature T:

$$\log \frac{t}{t_d} = \frac{E_{act}}{2.3R}\left(\frac{1}{T} - \frac{1}{T_d}\right),$$

where the subscript d denotes design values, R is the universal gas constant and E_{act} is the material-dependent activation energy. When the equation is evaluated for values of constant appropriate for PE ($E_{act} = 235,2$ kJ/mol) and we take $T_d = 310$ K, it appears that prosthesis service life is shortened almost by half when the temperature increases by 2K over the design value.

On the other hand, as pointed out by Lu and McKellop [33], at elevated temperatures the proteins present in the lubricant fluid in the experiments in vitro may precipitate forming a cushion shielding the bearing surfaces from wear and reducing the effect of the adhesive transfer of the polyethylene to metal surface. Unfortunately, with the soluble components precipitation, the lubricating quality of the fluid deteriorates.

4.1. Experimental techniques

Frictional heat generation has been investigated by various experimentalists in two distinct ways:

- In *vivo* measurements in patients. Bergmann et al. measured the temperature distribution and forces acting on the head of the implant by means of instrumented endoprosthesis, cf. [3]. For details the reader is referred to the paper by Bergmann et al in this volume.
- In *vitro* measurements of frictional torque, temperatures and material wear on a laboratory set-up over a prescribed range of joint motions.

Such a measurements were made by Davidson et al. [11, 12] and by Lu and McKellop [33]. Influence of the choice of material for articulating surfaces and a number of other parameters was studied. Some of the results are reviewed below.

In [11] the authors describe so called 'simulated in *vivo*' test where movement of the prosthesis is replaced by resistance heater embedded in the prosthetic head and the system is assembled in such a way as to resemble the real situation as much as possible (the joint capsule is simulated by pieces of bovine muscle tissue), therefore reproducing mechanisms of heat transport that occur in *vivo*. However, the effect of vascularity and blood flow is not reproduced in such a setup.

Materials of articulating surfaces have a marked influence on the heat production and rate of wear. In [11] and [12] the authors provide an extensive study of these issues. Three kinds of articulating pairs are taken into consideration (mentioned here in stem–acetabular cup order):

1. Co-Cr-Mo steel on UHMWPE (Ultra High Molecular Weight PolyEthylene),
2. alumina (Al_2O_3) on UHMWPE,
3. alumina on alumina.

Some of the results of *in–vitro* tests are displayed in Fig. 12 after [11]. Specialized test setup was used to produce rocking motion with variable hip loading. The profile of the loading during a single cycle is depicted in Fig. 13 after [11]. The load–time history was selected to reflect natural hip loading during walking. The results cover experiments conducted with two values of maximum force applied to femoral head, namely 2500 N and 5000 N.

The results presented in [33] show superior performance of alumina–UHMWPE, when compared to metal-UHMWPE pair *in-vitro*. Bergmann et al. [3] performed experiments which showed the superior performance of alumina–alumina articulation *in-vivo*.

The differences in heat production for various pairs come from different friction coefficients and can greatly influence wear performance of artificial joint. More detailed information about the rate of wear for different kinds of surfaces can be found in [12] and [16].

Another factor important for frictional heat generation is the lubrication. In natural joints it is accomplished by means of *synovial fluid*, liquid-crystalline, biological substance, see e.g. [59].

The available volume of synovial fluid in the joint capsule is less than 2 ml. It is a yellow, clear and highly viscous liquid. It forms a film layer of thickness varying on the type of joint and location within it, in range from 6 μm to 1mm. The synovial fluid in a healthy joint consists to 94% of water

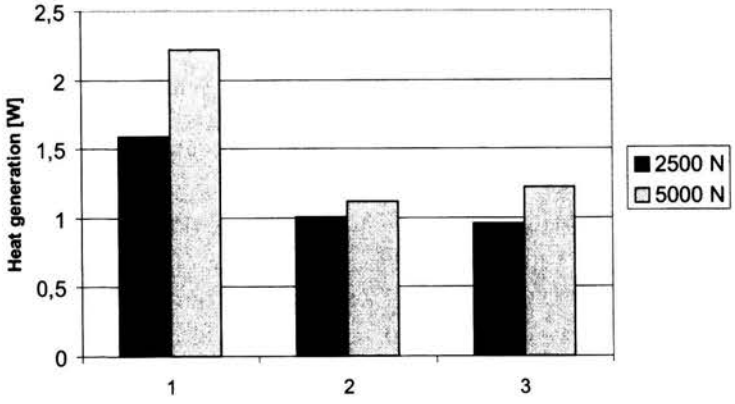

FIGURE 12. Heat generation for different articulating surfaces, after [11].

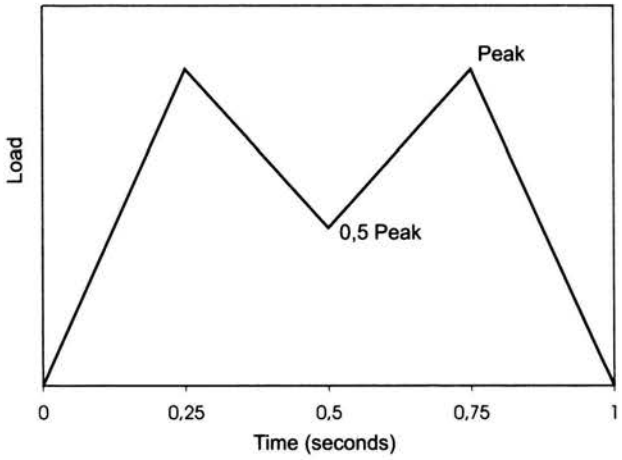

FIGURE 13. Walking load history, used in *in-vitro* frictional heating tests. Peak value was set to 2500 N or 5000 N, after [11].

and 2–3% of the hyaluronic acid by weight. Moreover, the synovial fluid contains some macromolecular components like glycoproteins, phospholipids and low molecular compounds, e.g. liquid crystalline cholesterol esters and small ions [59].

The main purpose of the synovial fluid is the lubrication of the joint. Furthermore, it provides the necessary nutrients for the cartillage and protects it from enzyme activity.

Properties of the synovial fluid are affected by pathological processes. The shear viscosity coefficient is smaller for synovial fluid from degenerated joints.

In natural joints the quality of the lubrication is strongly linked with the functioning of articular cartilage which can be treated as a multiphase porous material. For details the reader is referred to [23, 38].

In the *in-vitro* tests [12] the lubrication was attained by means of water or hyaluronic acid in different concentrations. The hyaluronic acid was chosen since it is the primary lubricant component of the synovial fluid. Additionally, friction in dry conditions as well as in the presence of 2 mg bone cement powder was investigated. No significant difference between water and hyaluronic acid lubrication was reported, while friction in dry conditions was, as expected, substantially greater. In Fig. 14 illustrative experimental relation is depicted between frictional torque in joint and lubrication conditions for steel–UHMWPE articulating pair [12]. To obtain these results hip simulator was used to create a rocking motion over a 46° range. The axial load variation was chosen to reflect the walking loads history, see [12] for details.

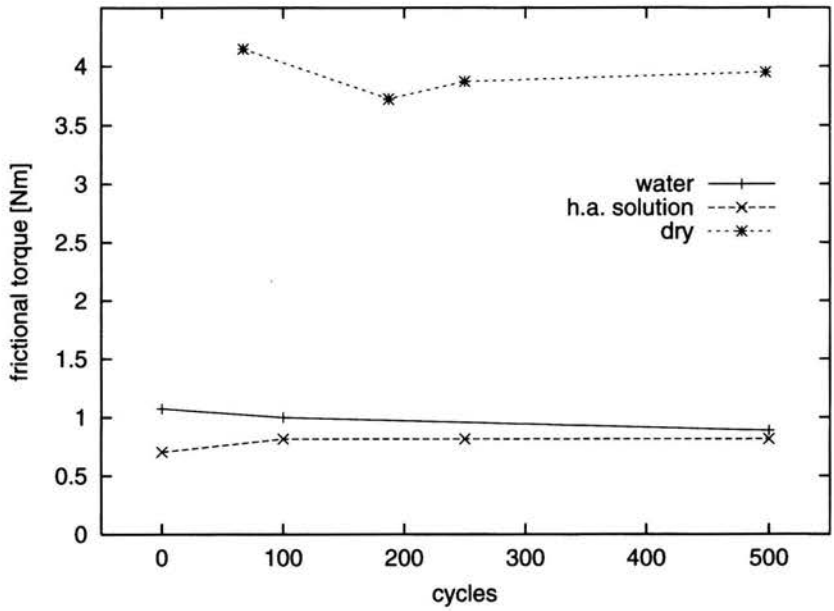

FIGURE 14. Frictional torque in lubricated and dry conditions. Peak hip load = 5000 N, after [12].

The frictional torque rises by an order of magnitude when bone cement is present in the joint, even in a small quantity. As results presented in [12]

indicate, there is an almost linear relation between frictional torque and equilibrium temperature rise.

A number of other factors influence the temperature distribution in joints. These are:

- Stride length and step frequency and consequently the flexion–extension angle and angular velocity, cf. [54].
- Adaptation. Bergmann et al. [3] reported that two patients with low measured temperatures in implanted joints had high body weight but were very active. This effect is assumed to have been caused by physiological adaptation of vascularity to higher temperatures (higher perfusion rates). It is, however, not always present.
- Possible head–acetabular cup separation during the joint movement. This effect is not present *in vivo*, where various supporting structures exist to restrain the femur head (fibrous capsule, acetabular labrum, ligament of the head of the femur and the iliofemoral, ischiofemoral, pubofemoral and transverse acetabular ligaments). During the total hip arthroplasty some of those structures may get surgically removed or resected to facilitate surgical exposure. The kinematics of the artificial joint is therefore different from the natural one. Measurements performed by Dennis et al. [14] prove that articulating surfaces separation occurs *in-vivo*. The influence of this effect on joint temperatures is not known but it is expected to be beneficial [3]. The gap that opens during the separation would be filled with synovial fluid, which would cool the articulating surfaces and the lubricating film would be renewed.

4.2. Modelling and simulation

Two basic properties of the frictional force F in a joint can be stated, cf. [20],

$$F \neq f(A), \quad F = \mu L$$

where A is the apparent area of contact, L is the normal load and μ is a number, termed the coefficient of friction. The second law, with μ being a constant is a good approximation in many cases. When the friction arises mainly from an adhesive mechanism, μ can be expressed as, cf. [20],

$$\mu \propto L^{\phi}$$

For purely elastic contact between the asperities theoretical value of ϕ is $-1/3$. In experimental studies the value of ϕ is greater because of plastic, as well as elastic, deformations of the asperities during the contact.

For the system with lubrication, the conditions of the friction are altered by the presence of fluid. Two regimes are generally distinguished here, cf. [20],

- *full fluid film lubrication*, The direct interaction between articulating surfaces is negligible. The frictional force arises only from the shear within the fluid. For a Newtonian fluid Hall and Unsworth [20] propose the following expression for μ:

$$\mu = \alpha \frac{\eta}{L} \frac{u}{h_c}.$$

  where u is the sliding velocity, η is the viscosity of the fluid and h_c denotes the central film thickness between articulating surfaces. The parameter α characterizes the contact regime.
- *Mixed lubrication.* The pressure in the film of lubricant is not enough to support the load and contact between the opposing surfaces occurs.

The simple engineering criterion for full fluid film lubrication to occur is that the surface separation ratio h_c/σ should exceed 3, where σ is the combined root mean square (RMS) surface roughness of the articulating surfaces [20].

In the hip joint the precise distribution of synovial fluid film thickness is not known and the frictional forces have contributions at different radii. Thus μ cannot be determined accurately from experimental data. Instead a friction factor is defined by the following equation:

$$T = fRL,$$

where T is the total frictional torque and L is the radius of the femoral head. The torque T is the driving force for the heat generation in joint.

The computer simulations of friction-induced heat dissipation are always considered in close connection with the experiment. Unlike in the case of bone cement polymerisation the stationary temperature field is usually considered, see [4]. This corresponds to the thermal equilibrium of the system when heat generation rate by friction equals the heat dissipation rate. This happens approximately after 1 hour of continuous walking (the half of total temperature increase taking place in the first 6 min.) according to in *vivo* measurements by Bergmann et al. [3]. Davidson et al. [12] reported half of this equilibration time for tests *in vitro*. Lu and McKellop [33] indicated much longer times (of the order of several hours) which is probably caused by different experimental protocol (much larger quantities of lubricant and lower forces in the joint).

The greatest difficulty of computer simulations seems to be the fact that one needs to choose the parameters for the model correctly and to do this

one needs to resort to some experimental data. The heat generation rate at the surface of contact of articulating components and thermal properties of tissues and synovial fluid must be obtained from experiments and experimental results show considerable scatter. Furthermore, if Fourier–Kirchhoff equation is used, the effect of vascularity is neglected or can be only roughly approximated.

In [4] Bergmann et al. conducted a finite element analysis of a stationary temperature field in the implant system. The geometry of the FEM model was reconstructed by the use of CT scans. Uniform heat generation rate at the implant head–acetabular cup interface was assumed and its value was chosen in such a way that the temperature profiles resembled as closely as possible the ones obtained experimentally. Then, the influence of the following factors was numerically investigated:

- the volume of synovial fluid,
- the perfusion rate in surrounding tissue,
- the possibility of separation between the femoral head and the acetabulum,
- friction conditions,
- thermal properties of individual elements of the system,
- the fixation technique (with or without cement),
- the size of the contact area between head and the cup.

Detailed results are described in [4].

Acknowledgement

The authors were partially supported by the State Commitee for Scientific Research (KBN, Poland) through the grants No 8T11F 017 18 and No 4 T11F 003 25. The first author was also supported by the grant No 4T11F 009 24 by the same institution.

References

1. B.R. BALIGA, P.L. ROSE, and A.M. AHMED, Thermal modeling of polymerizing polymethylmethacrylate, considering temperature-dependent heat generation. *J. Biomech. Eng.*, Vol.114, pp.251–259, 1992.

2. G. BERGMANN, F. GRAICHEN, and A. ROHLMANN, In vivo measurement of temperature rise in a hip implant. 37th Annual Meeting Orthopaedic Research Society.

3. G. BERGMANN, F. GRAICHEN, A. ROHLMANN, N. VERDONSCHOT, and G.H. VAN LENTHE, Frictional heating of total hip implants, Part 1: measurements in patients. *J. Biomech.*, Vol.34(4), pp.421–428, 2001.

4. G. BERGMANN, F. GRAICHEN, A. ROHLMANN, N. VERDONSCHOT, and G.H. VAN LENTHE, Frictional heating of total hip implants, Part 2: finite element study. *J. Biomech.*, Vol.34(4), pp.429–435, 2001.

5. N.E. BISHOP, S. FERGUSON, and S. TEPIC, Porosity reduction in bone cement at the cement-stem interface. *J. Bone Joint Surg. [Br]*, Vol.78(3), pp.349–356, 1996.

6. S. BIYIKLI, M.F. MODEST, and R. TARR, Measurements of thermal properties for human femora. *J. Biomed. Mat. Res.*, Vol.20, pp.1335–1345, 1986.

7. H.S. CARSLAW, J.C. JAEGER *Conduction of heat in solids.* Oxford University Press, 1954.

8. M.J. CHAMPAGNE, P. DUMAS, P. ORLOV, M.R. BENETT, P. HAMET, and J. TREMBLAY, Protection againts necrosis by heat stress proteins in vascular smooth muscle cells: Evidence for distinct modes of cell death. *Hypertension*, Vol.33, pp.906–913, 1999.

9. T. CHEN, R.P. KUSY, Effect of methacrylic acid:methyl methacrylate monomer ratios on polymerization rates and properties of polymethyl methacrylates. *J. Biomed. Mat. Res.*, Vol.36(2), pp.190–199, 1997.

10. R. CLATTENBURG, J. COHEN, S. CONNER, and N. COOK, Thermal properties of cancellous bone. *J. Biomed. Mat. Res.*, Vol.9, pp.169–182, 1975.

11. J.A. DAVIDSON, S. GIR, and J. PAUL, Heat transfer analysis of frictional heat dissipation during articulation of femoral implants. *J. Biomed. Mat. Res.*, Vol.22, pp.281–309, 1988.

12. J.A. DAVIDSON, G. SCHWARTZ, G. LYNCH, and S. GIR, Wear, creep, and frictional heating of femoral implant articulating surfaces and the effect on long-term performance–Part II: Friction, heating, and torque. *J. Biomed. Mat. Res.*, Vol.22, pp.69–91, 1988.

13. E.D. DAVIS, D.J. DOSS, J.D. HUMPHREY, N.T. WRIGHT, Effects of heat-induced damage on the radial component of thermal diffusivity of bovine aorta. *J. Biomech. Eng.*, Vol.122(3), pp.283–286, 2000.

14. D.A. DENNIS, R. KOMISTEK, E.J. NORTHCUT, J.A. OCHOA, and A. RITCHIE, *'In vivo'* determination of hip joint separation and the forces generated due to impact loading conditions. *J. Biomech.*, Vol.34(5), pp.623–629, 2001.

15. J.A. DIPISA, G.S. SIH, and A. BERMAN, A. The temperature problem at the bone-acrylic cement interface of the total hip replacement. *Clin. Orth.*, Vol.121, pp.95–98, 1976.

16. D. DOWSON, [Ed.], *Advances in Medical Tribology. Orthopaedic implants and implant materials.* Mechanical Engineering Publications Limited, London UK, 1998.

17. L.S. FLETCHER Recent developments in contact conductance heat transfer. *J. Heat Transfer*, Vol.110, pp.1059–1070, 1988.

18. S.B. GOODMAN, J. SCHATZKER, G. SUMNER-SMITH, V.L. FORNASIER, N. GOFTEN, and C. HUNT, The effect of polymethylmethacrylate on bone: an experimental study. *Arch. Orthop. Trauma. Surg.*, Vol.104(3), pp.150–154, 1985.

19. F. GRAICHEN, G. BERGMANN, and A. ROHLMANN, Hip endoprosthesis for *in vivo* measurement of joint force and temperature. *J. Biomech.*, Vol.32(10), pp.1113–1117, 1999.

20. R.M. HALL, A. UNSWORTH, Friction in hip prostheses. *Biomaterials*, Vol.18, pp.1017–1026, 1997.

21. N.J. HOLM, The formation of stress by acrylic bone cements during fixation of the acetabular prosthesis. *Acta Orth. Scan.*, Vol.51, pp.719–726, 1980.

22. R. HUISKES, Some fundamental aspects of human joint replacement. *Acta Orth. Scan.*, Vol.185, 1980.

23. J.M. HUYGHE, R. VAN LOON, F.T.P. BAAIJENS, P.M. VAN KEMENADE and T.H. SMIT, We are all porous media. [In:] *Poromechanics II*, J.-L. Auriault, C. Geindreau, P. Royer, J.-F. Bloch, C. Boutin, and J. Lewandowska, Eds. Balkema Publishers, Lisse, 2002.

24. W.L. JAFFEE, R.M. ROSE and E.L. RADIN, On the stability of the mechanical properties of self-curing acrylic bone cement. *J. Bone Jt. Surg., Am. Vol.*, Vol.56, pp.1711–1714, 1974.

25. C.D. JEFFERISS, A.J. LEE, R.S. LING, Thermal aspects of self-curing polymethylmethacrylate. *J. Bone Joint Surg. [Br]*, Vol.57(4), pp.511–518, 1975.

26. W.R. KRAUSE, D.M. BRADBURY, J.E. KELLY, and E.M. LUNCEFORD, Temperature elevations in orthopaedic cutting operations. *J. Biomech.*, Vol.15(4), pp.267–275, 1982.

27. R.P. KUSY, Characterization of self-curing acrylic bone cements. *J. Biomed. Mat. Res.*, Vol.12, pp.271–305, 1978.

28. E.P. LAUTENSCHLAGER, G.W. MARSHALL, Mechanical strength of acrylic bone cements impregneted with antibiotics. *J. Biomed. Mater. Res.*, Vol.10, pp.837–845, 1976.

29. A.J.C. LEE, R.S.M. LING, and S.S. VANGALA, The mechanical properties of bone cements. *J. Med. Eng. Tech.*, Vol.2, pp.137–140, 1977.

30. A.B. LENNON, P.J. PRENDERGAST, Residual stress due to curing can initiate damage in porous bone cement: experimental and theoretical evidence. *J. Biomech.*, Vol.35, pp.311–321, 2002.

31. A.B. LENNON, P.J. PRENDERGAST, M.P. WHELAN, R.P. KENNY, and C. CAVALLI, Modelling of temperature history and residual stress generation due to curing in polymethylmethacrylate. [In:] *Proceedings of the 12th Conference of the European Society of Biomechanics* (2000), P.J. Prendergast, A.J. Carr, and T.C. Lee, Eds., Royal Academy of Medicine in Ireland, Dublin, p. 253.

32. L. LINDER, Reaction of bone to the acute chemical trauma of bone cement. *J. Bone Joint Surg.*, Vol.59-A(1), pp.82–87, 1977.

33. Z. LU, H. MCKELLOP, Frictional heating of bearing materials tested in a hip joint wear simulator. [In:] *Advances in Medical Tribology. Orthopaedic implants and implant materials*, D. Dowson, [Ed.] Mechanical Engineering Publications Ltd, 1998, pp. 193–200.

34. L.S. MATTHEWS, C. HIRSCH, Temperatures measured in human cortical bone when drilling. *J. Bone Joint Surg. [Am]*, Vol.54(2), pp.297–308, 1972.

35. S. MAZZULLO, M. PAOLINI, and C. VERDI, Numerical simulation of thermal bone necrosis during cementation of femoral prostheses. *J. Math. Biol.*, Vol.29(5), pp.475–494, 1991.

36. L.G. MERCURI, Measurement of the heat of reaction transmitted intracranially during polymerization of methylmethacrylate cranial bone cement used in stabilization of the fossa component of an alloplastic temporomandibular joint prosthesis. *Oral Surg. Oral Med. Oral Pathol.*, Vol.74(2), pp.137–142, 1992.

37. D.D. MOSSER, J. DUCHAINE, L. BUORGET, and L.H. MARTIN, Changes in heat shock proteins synthesis and heat sensitivity during mouse thymocyte development. *Developmental Genetics*, Vol.14, pp.148–158, 1993.

38. V.C. MOW, A. RATCLIFFE, Structure and function of articular cartilage and meniscus. In: *Basic Orthopaedic Biomechanics*, V.C. Mow and W.C. Hayes, Eds. Lippincot-Raven Publishers, Philadelphia, 1997, pp. 113–177.

39. N. NUÑO, G. AVANZOLINI Residual stresses at the stem–cement interface of an idealized cemented hip system. *J. Biomech.*, Vol.35(6), pp.849–852, 2002.

40. M. OHTA, S. TSUTSUMI, S.H. HYON, Y.B. KANG, H. TANABE, Y. MIYOSHI, Residual stress measurements of ultra-high molecular weight polyethylene for artificial joints. *Rus.J. Biomech.*, Vol.4(2), pp.30–38, 2000.

41. E.M. ORTT, D.J. DOSS, E. LEGALL, N.T. WRIGHT, and J.D. HUMPHREY, A device for evaluating the multiaxial finite strain thermomechanical behavior of elastomers and soft tissues. *J. Appl. Mech.*, Vol.67, pp.465–471, 2000.

42. H.H. PENNES, Analysis of tissue and arterial blood temperatures in the resting human forearm. *J. Appl. Physiology*, Vol.1, pp.93–122, 1948.

43. P.J. PRENDERGAST, Biomechanical techniques for pre-clinical testing of prostheses and implants. Lecture notes at Centre of Excellence for Advanced Materials and Structures, Institute for Fundamental Technological Research, Polish Academy of Sciences, Warsaw, 2000.

44. N. RAMANIRAKA, Thermal bone necrosis at the bone-cement interface after cemented total hip arthoplasty: a finite element analysis. In: *12th Annual Meeting of the European Orthopaedic Research Society, Lausanne, Switzerland* (2002), P.F. Leyvraz, D. Pioletti, T. Quinn, and P. Zysset, Eds., pp. O–23.

45. F.W. RECKLING, W.L. DILLON, The bone-cement interface temperature during total joint replacement. *J. Bone Joint Surg.*, Vol.59-A(1), pp.80–82, 1977.

46. J. ROJEK, J.J. TELEGA, Contact problems with friction, adhesion and wear in orthopaedic biomechanics. Part I – General developments. *J. Theor. Appl. Mech.*, Vol.39(3), pp.655–677, 2001.

47. J. ROJEK, J.J. TELEGA, and S. STUPKIEWICZ, Contact problems with friction, adhesion and wear in orthopaedic biomechanics. Part II – Numerical implementation and application to implanted knee joints. *J. Theor. Appl. Mech.*, Vol.39(3), pp.679–706, 2001.

48. S. SAHA, S. PAL, Mechanical properties of the bone cement: A review. *J. Biomed. Mat. Res.*, Vol.18, pp.435–462, 1984.

49. M. SAITO, A. MARUOKA, T. MORI, N. SUGANO, and K. HINO, Experimental studies on a new bioactive bone cement: hydroxyapatite composite resin. *Biomaterials*, Vol.15(2), pp.156–160, 1994.

50. S.A. SAPARETO, W.C. DEWEY, Thermal dose determination in cancer therapy. *International Journal of Radiation Oncology Biology Physiology*, Vol.10, pp.787–800, 1984.

51. J. SCHATZKER, J.G. HORNE, G. SUMNER-SMITH, R. SANDERSON, and J.P. MURNAGHAN, Metylmethacrylate cement: its curing temperature and effect on articular cartilage. *Canadian J. Surg.*, Vol.18, pp.172–178, 1975.

52. Y. SENAHA, T. NAKAMURA, J. TAMURA, K. KAWANABE, H. IIDA, and T. YAMAMURO, Intercalary replacement of canine femora using a new bioactive bone cement. *J. Bone Joint Surg.*, Vol.78(1), pp.26–31, 1996.

53. A. SHITZER, S. BELLOMO, L.A. STROSCHEIN, R.R. GONZALEZ, and K.B. PANDOLF, Simulation of a cold-stressed finger including the effects of wind, gloves and cold-induced vasodilatation. *J. Biomech. Eng.*, Vol.120, pp.389–394, 1998.

54. A.V. SOTIN, Y.V. AKULICH, and R.M. PODGAYETS, The calculation of loads ating on the femur during normal human walking. *Rus.J. Biomech.*, Vol.4(1), pp.49–61, 2000.

55. P. SPENCER, C.M. COBB, D.M. WIELICZKA, A.G. GLAROS, and P.J. MORRIS, Change in temperature of subjacent bone during soft tissue laser ablation. *J. Periodontol.*, Vol.69(11), pp.1278–1282, 1998.

56. M. STAŃCZYK, J.J. TELEGA, Thermal problems in artificial joints: influence of bone cement polymerization. *Acta Bioengng. Biomech.*, Vol.3, pp.489–496, 2001.

57. M. STAŃCZYK, J.J. TELEGA, Modelling of heat transfer in biomechanics – a review. part I. Soft tissues. *Acta Bioengng. Biomech.*, Vol.4(1), pp.31–61, 2002.

58. L.W. SWENSON JR, D.J. SCHURMAN, and R. PIZIALI, Finite element temperature analysis of a total hip replacement and measurement of PMMA curing temperatures. *J. Biomed. Mat. Res.*, Vol.15(1), pp.83–96, 1981.

59. E. SZWAJCZAK, A. KUCABA-PIĘTAL, and J.J. TELEGA, Liquid crystalline properties of synovial fluid. *Engng Trans.*, Vol.49, pp.315–358, 2001.

60. K. TAKEGAMI, T. SANO, H. WAKABAYASHI, J. SONODA, T. YAMAZAKI, S. MORITA, T. SHIBUYA, and A. UCHIDA, New ferromagnetic bone cement for local hyperthermia. *J. Biomed. Mat. Res.*, Vol.43(2), pp.210–214, 1998.

61. S. TEPIC, T. MACIROWSKI, and R.W. MANN, Experimental temperature rise in human hip joint in vitro, in simulated walking. *J. Orthop. Res.*, Vol.3, pp.516–520, 1985.

62. S. TOKSVIG-LARSEN, H. FRANZEN, and L. RYD, Cement interface temperature in hip arthoplasty. *Acta Orth. Scan.*, Vol.62(2), pp.102–105,1991.

63. S. TOKSVIG-LARSEN, L. RYD, and A. LINDSTRAND, On the problem of heat generation in bone cutting. *J. Bone Joint Surg. [Br]*, Vol.73(1), pp.13–15, 1991.

64. S. TOKSVIG-LARSEN, L. RYD, and A. LINDSTRAND, Temperature influence in different orthopaedic saw blades. *J. Arthoplasty*, Vol.7(1), pp.21–24, 1992.

65. A. TONI, F. TRAINA, B. BORDINI, S. STEA, S. PADERNI, and A. GIUNTI, Cemented versus cementless stem-to-bone fixation: a long term survival comparison with an identical prosthetic design and ceramic on ceramic coupling. In: *12th Annual Meeting of the European Orthopaedic Research Society, Lausanne, Switzerland* (2002), P.F. Leyvraz, D. Pioletti, T. Quinn, and P. Zysset, Eds., pp. O–84.

66. B. VÁZQUEZ, M.P. GINEBRA, F.J. GIL, J.A. PLANELL, A. LÓPEZ BRAVO, and J. SAN ROMÁN, Radiopaque acrylic cements prepared with a new acrylic derivative of iodo-quinoline. *Biomaterials*, Vol.20, pp.2047–2053, 1999.

67. S. WEINBAUM, L.M. JIJI, A new simplified bioheat equation for the effect of blood flow on local average tissue temperature. *J. Biomech. Eng.*, Vol.107, pp.131–139, 1985.

68. M.P. WHELAN, R.P. KENNY, C. CAVALLI, A.B. LENNON, and P.J. PRENDERGAST, Application of the optical fibre Bragg grating sensors to the study of PMMA curing. In: *Proceedings of the 12th Conference of the European Society of Biomechanics* (2000), P.J. Prendergast, A.J. Carr, and T.C. Lee, Eds., Royal Academy of Medicine in Ireland, Dublin, p. 252.

69. H.G. WILLERT, J. LUDWIG, and M. SEMLITSCH, Reaction of bone to methacrylate after hip arthoplasty. *J. Bone Joint Surg.*, Vol.56-A(7), pp.1368–1382, 1974.

70. S. WIŚNIEWSKI, T. WIŚNIEWSKI, *Heat transfer (in Polish)*. Wydawnictwa Naukowo Techniczne, Warszawa, 1997.

71. Y.L. WU, S. WEINBAUM, and L.M. JIJI, A new analytic technique for 3-D heat transfer from a cylinder with two or more axially interacting eccentrically embedded vessels with application to countercurrent blood flow. *J. Heat Mass Transfer*, Vol.36(4), pp.1073–1083, 1993.

72. A.G.M. WYKMAN, Acetabular cement temperature in arthroplasty. Effect of water cooling in 19 cases. *Acta Orth. Scan.*, Vol.63(5), pp.543–544, 1992.

73. T.H. YOUNG, C.K. CHENG, Y.M. LEE, L.Y. CHEN, and C.H. HUANG, Analysis of ultrahigh molecular weight polyethylene failure in artificial knee joints: Thermal effect on long-term performance. *J. Biomed. Mat. Res.*, Vol.48(2), pp.159–164, 1999.

74. M. ZHU, S. WEINBAUM, and L.M. JIJI, Heat exchange between unequal countercurrent vessels asymetrically embedded in a cylinder with surface convection. *J. Heat Mass Transfer*, Vol.33(10), pp.2275–2284, 1990.

75. M. ZHU, S. WEINBAUM, and D.E. LEMONS, A three-dimensional variable geometry countercurrent model for whole limb heat transfer. *J. Biomech. Eng.*, Vol.114(3), pp.366–376, 1992.